

Detailed analysis of the influence of coronal mass ejections on the ionosphere with amateur equipment

Wolfgang Kaufmann, DL1WKA, contact(at)ars-electromagnetica.de, Sept. 2024

Introduction

The use of databases on radio links provided by radio amateurs (WSPRNet, RBN, PSKReporter) is also recognised and used in professional ionospheric research [1]. The question to be investigated here is what statements can be made about the changes in the state of the ionosphere when the Earth is hit by a coronal mass ejection (CME) using amateur means. The coupling of solar plasma into the terrestrial magnetosphere not only triggers a disturbance of the terrestrial magnetic field (geomagnetic storm) but also a significant decrease in the electron density in the F2 layer. From the observation of a reduced reflection height of VLF waves at the D layer, an increase in electron density at an altitude of 70-80 km can also be inferred [2]. These ionospheric effects are known as ionospheric storm. The ionospheric disturbances persist for several days after the geomagnetic activity has normalized.

The 40 m band (~ 7 MHz) was chosen to investigate this issue. In this band the propagation of radio waves reacts very sensitively to the electron density of both the absorbing D-layer and the reflecting F2-layer. The start, strength and duration of a possible ionospheric storm are naturally not yet known at the start of an investigation. Instead of continuous monitoring, three separate measurements were therefore carried out: before, during and after an ionospheric storm. It was possible to include the extremely strong solar storm of May 11, 2024. In addition to the CME, this period was also characterized by the occurrence of some very strong solar X-ray bursts and an increased solar proton flux, see Fig. 1.

Methods

The digital beacon protocol “WSPR” developed by Joe Taylor was used as a “measuring tool”. With the help of the WSPR database “wspnet.org”, which is accessible via the Internet, own WSPR transmissions can be tracked worldwide. For this study, only the reports of the own transmitted WSPR signals were used for analysis. This ensured that the same technical TX conditions were always used. It also allowed the entire transmission planning to be tailored to the requirements of the intended investigation. The TX location was Algermissen, northern Germany. The WSPR

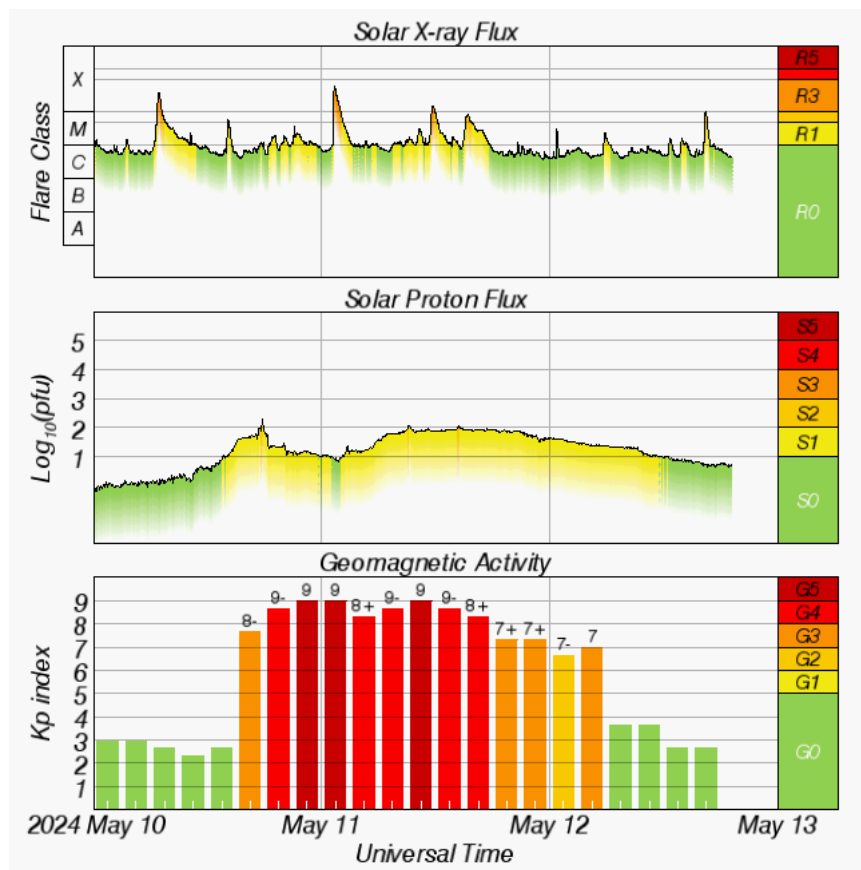


Fig. 1: Space weather conditions from 10 to 12 May 2024, courtesy of NOAA/NWS, Space Weather Prediction Center.

beacon signals were transmitted every 10 minutes by an ICOM IC-7300. The EIRP was 5 W. The antenna used was a loaded broadband antenna (Diamond BB6WS). The observation periods are listed in Table 1.

Tab.1: Date and time in UTC for the three measurement periods.

Start	End	Solar Flux (10.7 cm) [s.f.u.]
2024-05-05 16:00	2024-05-07 16:30	174-207
2024-05-10 17:00	2024-05-16 16:00	212-228
2024-07-24 19:00	2024-07-31 02:00	172-230

Disturbances of the Earth's magnetic field and ionospheric disturbances are caused by the same solar outburst event. Luckily, the geomagnetic activity can be measured directly and provides information about the strength of the influence of a CME on the Earth (and thus also on the ionosphere). The linear three-hourly ap index was chosen as a measure of the geomagnetic disturbance. The numerical values of the ap index and the solar flux as a measure of solar activity were taken from [3]. A list of X-ray flares was compiled from [4]. The critical frequency of the F2 layer was taken from [5] for the "Juliusruh" ionosonde in northern Germany.

Results

The results of the measurement campaign are presented in the form of kernel density diagrams [6]. Using a suitable mathematical function (kernel), a two-dimensional density map is calculated from the logarithm of TX-RX distance and the time of the individual WSPR reports. This form of representation makes it possible to recognise significant changes in the time- and distance-dependent report density.

Firstly, the density map of the July measurements will be considered as a reference for a largely undisturbed temporal and spatial distribution of the WSPR reports. Fig. 2 shows a recurring distribution pattern depending on the time of day. It is the result of the interaction of the daily variation of the electron density of the D and F2 layer in combination with the geographical distribution of the RX stations (Europe and to a lesser extent North America). The attenuating effect of the D-layer increases as the angle of incidence decreases (lengthening of the path in the D-layer). This favours connections with short to medium range in the 40 m band during the day. At night, the D-layer disappears. After midnight, the cut-off frequency of the F-layer reaches its lowest point (see below). The lower the critical frequency, the lower the angle of incidence must be for reflection to occur. Under these conditions, long-range radio connections are favoured. In the 40 m band, this diurnal interaction of the D and F layers led to two characteristic density gaps, one defined by the time of the dip in the number of short-range connections (tSD), Fig. 2 dotted line A, and the other by the time of the dip in the number of long-range connections (tLD), Fig. 2 dotted line B. tSD is at 03:00 UTC and tLD at 12:00 UTC.

Fig. 2 also shows the weak influence of two short-term geomagnetic disturbances with ap indices around 50 (event no. 1 and 2) during . The increase in the ap index is accompanied by a simultaneous decrease in the number of radio connections at the longer distances (see arrow marks). This indicates a temporary reduction in the critical frequency of the F layer.

The next step will be an analysis of the situation before and during the extremely strong geomagnetic storm on 11 May, see Fig. 3:

(1) The most striking phenomenon here is the radio blackout that lasted more than 24 hours during the geomagnetic storm, Fig. 3 event no. 2. The blackout is not limited to daylight hours, but also persists during the night.

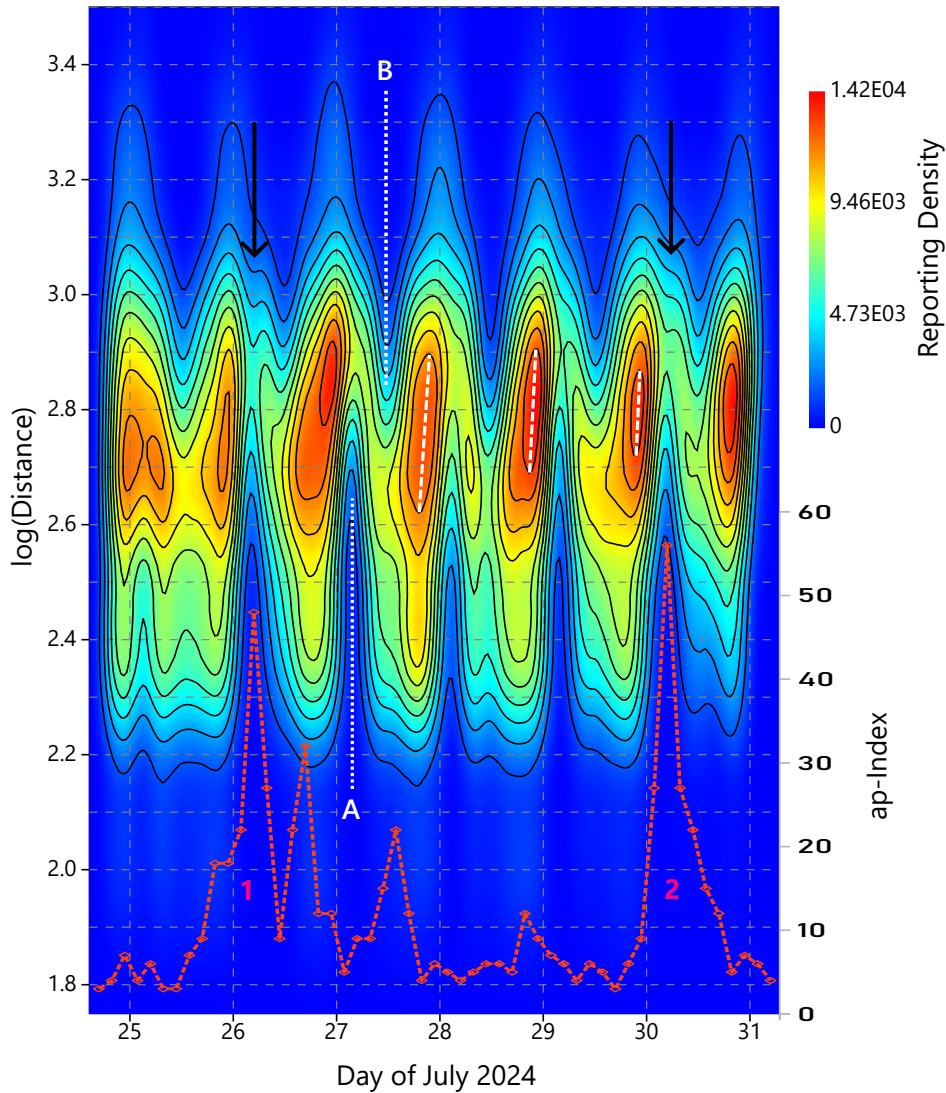


Fig. 2: Kernel density diagram of the received reports per time and logarithm of distance in July 2024. A kernel with a triangular function was used. The ap index is shown in purple. The geomagnetic events are numbered 1 and 2.

(2) In addition, two smaller geomagnetic disturbances of short duration could be observed, Fig. 3 events No. 1 and 3. During these periods, a significant, longer lasting decrease in the density of short-range connections was observed, see Fig. 3 white arrows.

3) The parameters tSD and tLD determined during the reference measurement remain unchanged at 03:00 UTC and 12:00 UTC respectively. Three days after storm event no. 2, however, the density gap at tSD on 15 May is not detectable, see Fig. 3 dotted line A. The report density centre on 14 May is also at 24:00 UTC with the axis inclined to the left (Fig. 3 dashed line). This is in contrast to the results of the reference measurement with daily report density centres at 21:30 UTC and axes inclined to the right (Fig. 2 dashed lines). Also, the centre of the report density centre on this day is about 100 km lower than on 6 May, immediately before the geomagnetic storm.

A series of X-class X-ray bursts occurred during the measurement campaign. They led to brief radio blackouts during the daylight hours. However, these short-term events have no noticeable effect on the density maps.

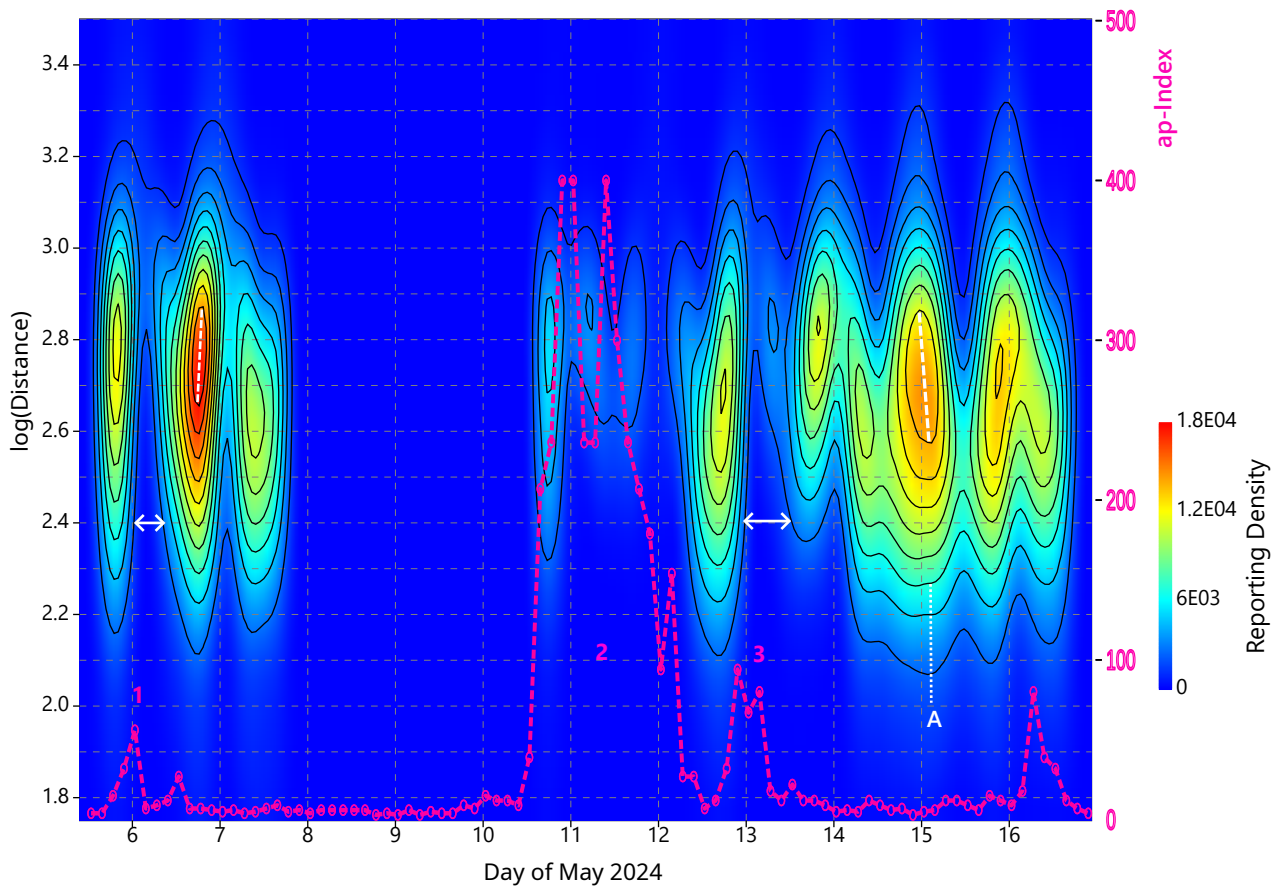


Fig. 3: Kernel density diagram of the received reports per time and logarithm of distance in May 2024. A kernel with a triangular function was used. The ap index is shown in purple. The geomagnetic events are numbered from 1 to 3. No measurements were taken in the period 7 May, 16:30 to 10 May, 17:00 UTC (see Table 1).

Discussion

The D region is the centre of absorption of high-frequency waves. Its presence and electron density are under strong solar control and normally disappear during the night. During and after a geomagnetic storm, the influx of electrons from the outer Van Allen belt is thought to be responsible for the increase in electron density in the D region [2].

The electron density of the F2 layer is dependent on solar radiation and its critical frequency varies with the time of day. The electron density of the F-layer passes through a minimum during the night, see Fig. 4. During a geomagnetic storm, a reduction in the electron density of the F-layer is known. The current assumption is that there is an influx of high energy ions from the ring current, which heats up the ionosphere and influences the high wind currents [2].

Taking into account the fact that the D and F2 layers affect radio waves with flat angles of incidence in opposite ways, some conclusions can be drawn from the density map about the underlying changes in the electron densities of the D and F layers.

When interpreting the finding (1), it is unclear what role an increased electron density of the D-layer and the lowering of the critical frequency of the F2-layer played in the 7 MHz radio blackout on 11 May. The ionosonde in Juliusruh, northern Germany, was fully functional during this period

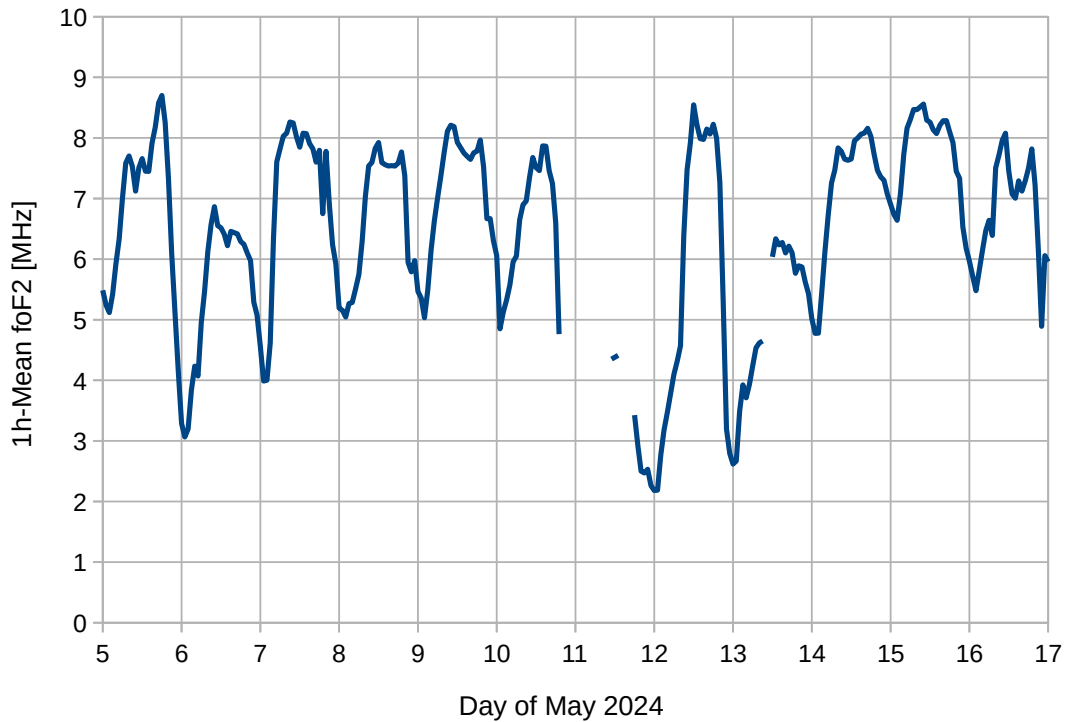


Fig. 4: Hourly average of the critical frequency of the F2 layer in May 2024, foF2, measured by the Juliusruh ionosonde, northern Germany

(it registered the E layer), but has no foF2 recordings, see Fig. 4. This indicates a massive loss of electron density in the F2 layer. The few remaining radio connections could be due to reflections from ionospheric irregularities.

Finding (2) showed that short report distances were largely absent during the geomagnetic disturbances, while the report density at long distances was not affected. This can be interpreted as a sign of a temporary reduced critical frequency of the F-layer. Indeed, Fig. 4 shows a lower value than usual for foF2 at the beginning of 6 and 13 May.

Finding (3): The lack of a short-range minimum at tSD indicates that the nocturnal drop in the electron content of the F-layer was lower than usual. This assumption is confirmed by the ionosonde measurement, see Fig. 4. The shift of the report density centre towards midnight and towards shorter report distances can be interpreted as a consequence of the high nocturnal ionisation density of the F-layer. Statistical analyses of the course of ionospheric storms [2] show that such one-off increases in ionisation density beyond the normal state occur in the recovery phase of the ionosphere.

To summarise, it can be said that ‘WSPR’ as a ‘measuring tool’ is capable of providing a finely resolved representation of ionospheric state changes that are in complete agreement with the results of ionosonde measurements.

References

- [1] Heliophysics and amateur radio: citizen science collaborations for atmospheric, ionospheric, and space physics research and operations. / Frissell, Nathaniel A.; Ackermann, John R; Alexander, Jesse N. et al. In: *Frontiers in Astronomy and Space Sciences*, Vol. 10, 16.11.2023.
- [2] Hargreaves J.K.: *The solar-terrestrial environment*. Cambridge University Press 1992

[3] Helmholtz-Zentrum Potsdam, Deutsches GeoForschungsZentrum GFZ (<https://kp.gfz-potsdam.de/daten>)

[4] NOAA/NWS, Space Weather Prediction Center (<ftp://ftp.swpc.noaa.gov/pub/warehouse/>)

[5] Lowell GIRO Data Center (<https://giro.uml.edu/>)

[6] Hammer Ø., Harper D. A. T., and Ryan P. D. (2001). "PAST: Paleontological statistics software package for education and data analysis". *Palaeontologia Electronica*, 4:1, 9pp.